Journal of Thermal Analysis and Calorimetry (2019) 137:1797–1807
https://doi.org/10.1007/s10973-019-08076-0

An experimental study on MWCNT–water nanofluids flow and heat transfer in double-pipe heat exchanger using porous media

Ahmad Moradi[1] · Davood Toghraie[2] · Amir Homayoon Meghdadi Isfahani[1] · Ali Hosseinian[1]

Received: 16 November 2018 / Accepted: 6 February 2019 / Published online: 20 February 2019

Abstract
This paper presents the results of an experimental investigation on the heat transfer characteristics of multi-walled carbon nanotube aqueous nanofluids inside a countercurrent double-pipe heat exchanger using porous media. Aluminum porous media (ε=67%) were used because of the construction of the medium, with porous plate media at the center of the inner tube and with three porous plates on the walls of the inner tube. The effects of operating parameters including flow rate (4600<Re<7600), mass fractions of nanofluids (0.04–0.25 mass%), and inlet temperature of nanofluids (Tin=50 °C) on the heat transfer coefficient were investigated. The results indicate that imposing the plate porous media increases the heat transfer coefficient significantly, and the highest increase in the heat transfer coefficient is 35% which is obtained in the test of the lowest mass fraction (0.04 mass%) with three-plate porous media in the experiment range. As the mass fractions increased, the value of heat transfer enhancement assisted by porous media gradually decreased. Also the lower range 100 (L h^{-1}) of the volume flow rate has a powerful enhancement on the enhancement coefficient, while the higher ranges 300 (L h^{-1}) have low influence.

Keywords Heat transfer enhancement · Multi-walled carbon nanotube · Porous media · Double-pipe heat exchanger

List of symbols

A	Heat transfer area (m^2)
D, d	Diameter (m)
K	Thermal conductivity (W m^{-1} °C^{-1})
C_p	Specific heat (J kg^{-1} °C^{-1})
Re	Reynolds number
T	Fluid temperature (°C)
T_w	Wall temperature (°C)
LMTD	Log mean temperature difference (°C)
U	Overall heat transfer coefficient (W m^{-2} °C^{-1})
h	Heat transfer coefficient (W m^{-2} °C^{-1})
m	Volume flow rate (m^3 s^{-1})
$\dot{m}$	Mass flow rate (kg s^{-1})
Nu	Nusselt number
Pr	Prandtl number

Greek letters

μ	Dynamic viscosity (kg m^{-1} s^{-1})
ρ	Fluid density (kg m^{-3})
mass%	Mass fraction

Subscripts

w	Wall
c	Cold
h	Hot
i	Inlet
o	Outlet
in	Inter
out	Outer
ip	Inlet of pipe
ave	Average
b	Bulk

✉ Davood Toghraie
Toghraee@iaukhsh.ac.ir

[1] Department of Mechanical Engineering, Najafabad Branch, Islamic Azad University, Najafabad, Iran

[2] Department of Mechanical Engineering, Khomeinishahr Branch, Islamic Azad University, Khomeinishahr 84175-119, Iran

Introduction

The nanofluid technology offers a high potential for controlling the heat transfer systems and increasing heat exchange efficiency in small volumes. Fluid properties can improve with addition of nanomaterials. In some cases such as where it is necessary to transfer high thermal flux from the solid environment to the fluid, existing methods such as modifying the fluid dynamics, flow geometry alone could not handle the rising energy control demand in existing processes. Accordingly, it is necessary to increase the efficiency of these applications while optimizing energy consumption and decreasing operating costs.

Many attempts have been made to increase heat transfer rates using nanofluids [1–4]. Most of these experiments are water-based nanofluids in heat exchangers and show an increased heat transfer coefficient compared to pure water [5, 6]. Many other investigations employ double-pipe heat exchangers [7–16]. Ding et al. [17] performed an experimental study on the laminar flow and heat transfer of nanofluids in a tube, confirming greater heat transfer coefficient of nanofluids over pure water. The enhancement also further depends on the flow conditions, nanoparticle's volume fraction, and the pH suspension. Sarafraz et al. [18] investigated the flow and heat transfer of nanofluids inside a heat exchanger. Forced convection experiments were performed in laminar and turbulent flow regimes, demonstrating that nanoparticles can enhance the thermal conductivity by up to 56%. Multi-walled carbon nanotube (MWCNT) with high thermal conductivity has attracted the attention of researchers [19–21]. Akhavan-Behabadi et al. [22] performed an experimental investigation on rheological properties and heat transfer characteristics of nanofluid flow through vertical tubes. They found that the heat transfer coefficient of nanofluid is higher than heat transfer coefficient of the base fluid. Their results showed significant heat transfer enhancement for nanofluids compared to base fluids. Huang et al. [23] studied heat transfer characteristics of nanofluids. They demonstrated that the heat transfer can be improved by using of nanofluids. Diao et al. [24] investigated the flow and heat transfer of nanofluids in minichannels. They found that the friction factor and Nusselt number of nanofluids are higher than friction factor and Nusselt number of water.

In recent years, the analysis of the nanofluid flow and heat transfer in porous media have been considered by researchers with interests in mechanical applications, including heat exchangers, boilers, nuclear flasks. Porous media increase the heat transfer surface area by changing the fluid regime from laminar to turbulent, increasing fluid velocity. Recently, Karimipour-Fard et al. [25] studied numerically the heat transfer enhancement of a heat exchanger by porous media. Their results showed that by using porous media, the cooling rate can improved by approximately 40%. The various works on natural convection can be mentioned like Chamkha et al. [26], Bourantas et al. [27], Sheremet et al. [28], and Uddin and Harmand [29]. Research on forced convection of nanofluids by Armaghani et al. [30], Nasrin et al. [31, 32] and Kasaeian et al. [33] shows the dependency of nanofluid flow in porous media on nanoparticle volume fraction and nanoparticle type. These parameters can further increase the Nusselt number value as well an increase in heat transfer rate. Pavel et al. [34] studied, experimentally and numerically, the effect of porous media on the heat transfer rate. They reported that porosity and the porous radius ratio have a positive effect on the heat transfer rate and have a negative effect on the pressure drop. Mohamad [35] investigated the laminar flow in porous media. He showed that partially filling the channel has better heat transfer and pressure drop characteristics than fully filled channels, also with porous media can reduce the thermally developing length by 50% or more. In another work, Targui and Kahalerras [36] studied the heat transfer performance in a heat exchanger with porous structures. The effects of Darcy number, porous thickness, and thermal conductivity ratio were considered. According to their results, the highest average Nusselt number ratio was obtained at low permeability and high thicknesses of the porous media. The enhancement of heat transfer rate using porous media and nanofluids simultaneously in a heat exchanger has rarely been studied and published. This paper examines the heat transfer of the MWCNT–water nanofluids in a double-pipe heat exchanger made of PVDF tube. It also includes the effects of porous media on flow and heat transfer characteristics at various volume flow rates and mass concentrations.

Experimental

Experimental setup

The schematics of experimental setup used in this investigation are shown in Fig. 1. This setup consists of a double-tube countercurrent flow heat exchanger, a heating unit to heat the working fluid, a temperature measurement system, two fluid circulation units, and measurement instruments. To measure the inlet and outlet temperatures of the working fluid, two RTD thermometers and four k-type thermocouples are used. The experimental system was isolated with glass wool insullation to prevent environmental heat losses. An electric heater with a thermostat is used to maintain the temperature of the nanofluid. Two flowmeters were installed in the pipes carrying nanofluid to check the flowing rate. Deionized water is the working fluid for the outer tube and MWCNT–water nanofluid is the working fluid for inner tube. The stainless steel tanks are used to store the nanofluid and cold water. For each fluid circulation, a centrifugal pump was employed to circulate the fluid inside the system. Table 1 details the accuracy of instruments. The temperature of nanofluid was set at 35–50 °C, and volume flow rates of nanofluid were adjusted at

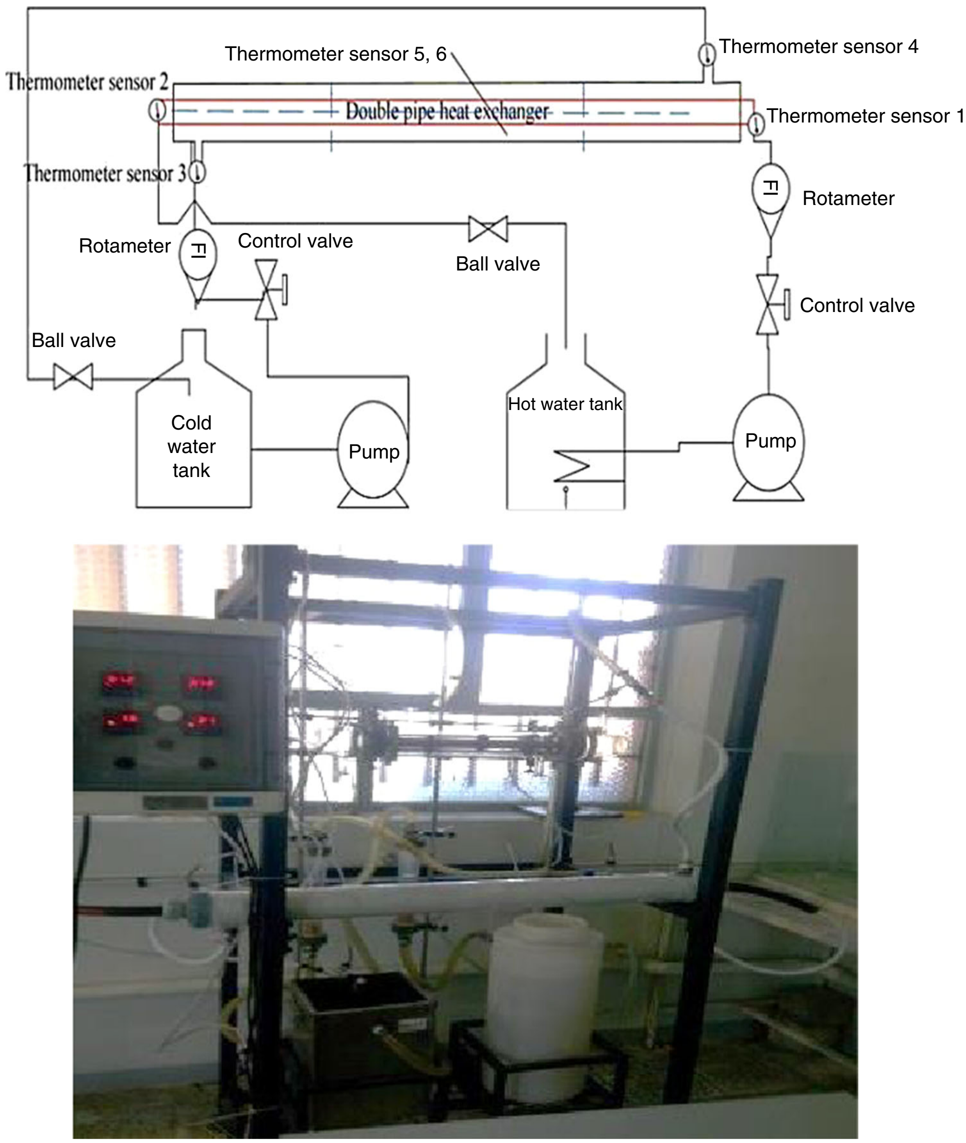

Fig. 1 Experimental setup

100, 200, 300 (L h^{-1});, and 300 (L h^{-1}) for the cold water flow rate. Three sets of experiments were performed to ensure the repeatability and consistency of results in presence of porous media.

The components of heat exchanger were constructed of 900 mm length, 84-mm outside-diameter tube and 19-mm inner tube. The inner tube was of copper composition, while the outside tube was made of PVDF. Table 2 shows the specifications of the heat exchanger.

The porous media in this study are open-cell aluminum plates with ε=67% nominal porosity. Figure 2 shows a schematic of porous media plate used in double-pipe heat exchanger. The three interrupted-plate designs have a nominal plate thickness of 0.8 mm and a nominal plate diameter of 83.5 mm, density of 2770 kg m^{-3}, and thermal conductivity of 205 (W m^{-1} °C^{-1}) At an altitude of 70 mm, the plates have a cut in the upper part to improve mixing of exterior fluid flow. As shown in Fig. 3. The spacing of the inter-plate in the length of heat exchanger tube is divided into three equal parts (approximately 300 mm) which are set in the opposite direction (Fig. 3).

Nanofluid preparation

For nanofluid preparation, deionized water (DIW) was used as the base fluid MWCNT (USNANO research Co.) was used as nanoparticle (see Table 3). Nanofluids were prepared at different mass fractions of 0.04%, 0.17%, 0.25%. Figure 4 demonstrates the transmission electron microscopy (TEM) image of the MWCNT nanoparticles. Figure 4 shows the quality of MWCNT, which shows that there is no impurity in structure of MWCNT. MWCNTs

Table 1 Details of measuring instruments

Instrument	Model	Accuracy
Rotameter	Glass tube Teflon	2% of readings[b]
RTDs	PT-100 resistance sensor	0.1 °C
Thermocouple	Type K	0.1 °C
Bolt heater	1200 W, 100 mm × 10 mm (L × D)	± 2% of readings[a]
Pump	Centrifugal, stainless steel impeller	–
Thermophysical properties		
Viscosity	Brookfield	2.5% of readings[b]
Thermal conductivity	Decagon KD2-Pro	2.5% of readings[b]

[a]Based on the calibration process

[b]Based on manufacturer claim

were initially dispersed into the water using 40 kHz and 300 W ultrasonic. The CTAB surfactant was used at only 0.1% of general volume of nanofluids.

Figure 5 shows the effect of surfactant on nanofluid stability. This figure shows that MWCNTs quickly settled down without the use of proper dispersant and it was dispersed and suspended well in the water with the CTAB surfactant. At maximum mass concentrations (mass%=0.25), nanofluids were stable for about 25 days.

Fig. 2 Schematic of the porous media plate used in this work

Calculation steps

Evaluation of overall heat transfer coefficient

For our purposes here, two mass flow rates are defined; the mass flow rate for the hot fluid inside the inner tube ($\dot{m}_h$) and a second mass flow rate for the coolant ($\dot{m}_c$). These mass flow rates exhibited as:

$$\dot{m}_h = m_h \times \frac{\rho_h}{3600000} \quad \dot{m}_c = m_c \times \frac{\rho_c}{3600000} \tag{1}$$

where $\dot{m}_h$ and $\dot{m}_c$ are the mass flow rates of the hot and cold fluids, respectively. ρ_h and ρ_c indicate hot and cold fluid densities, respectively. Heat transfer from hot fluid to cold fluid (Q_h) and from the cold fluid to hot fluid (Q_c) are calculated from the following formula [37],

$$Q_h = \dot{m}_h \times C_{p,h}\left(T_{in,h} - T_{out,h}\right), \quad Q_C = \dot{m}_c \times C_{p,c}\left(T_{out,c} - T_{in,c}\right) \tag{2}$$

where $C_{p,h}$ is specific heat for hot fluid and $C_{p,c}$ is specific heat for coolant. The average heat transfer rate can be expressed in the following manner:

$$Q_{avg} = \frac{Q_h + Q_c}{2} \tag{3}$$

The convective heat transfer coefficient h_i can be calculated from the following equation:

$$h_i = \frac{Q_h}{A_{is,ip} \times \left(T_w - T_{avg,h}\right)} \tag{4}$$

where $A_{is,ip}$ is the internal surface area of inner tube, T_w is the local surface temperature at the outer wall of the inner tube and $T_{avg,h}$ is average temperature of hot fluid. The Nusselt number is determined from the following formula:

$$\mathrm{Nu}_h = \frac{h_i \times D_h}{k_h} \tag{5}$$

where k_h is the thermal conductivity of the hot fluid and D_h is hydraulic diameter for hot flow. Logarithmic mean temperature difference is given by:

$$\mathrm{LMTD} = \frac{(T_{hi} - T_{co}) - (T_{ho} - T_{ci})}{\ln\left\{\frac{(T_{hi} - T_{co})}{(T_{ho} - T_{ci})}\right\}} \tag{6}$$

Experimental overall heat transfer coefficient (based on inner surface area of inner pipe) is evaluated from the following equation [38]:

Table 2 Specifications of the heat exchanger tubes

	Material	Inner diameter/mm	Thickness/mm	Length/cm
Inner tube	Copper	19	2	87.5
Outer tubes	PVDF	84	4	87.5

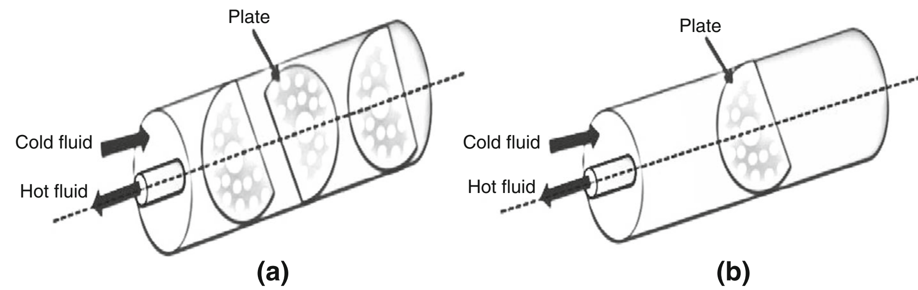

Fig. 3 Arrange of porous media plates: **a** three plates; **b** one plate

Table 3 Specification of MWCNT

Nanomaterial	MWCNT
Thermal conductivity/W m^{-1} °C^{-1}	>3000
Outside diameter/nm	5–15
Inside diameter/nm	3–5
Length/um	50
Color	Black
Purity/%	>95
Density/g cm^{-3}	2.1

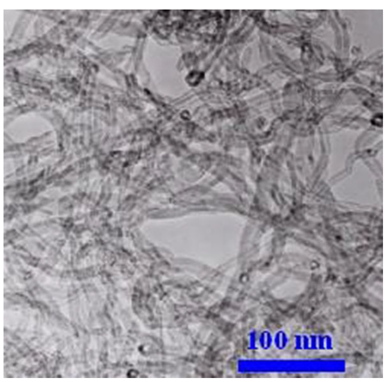

Fig. 4 Scanning electron microscopy of produced MWCNTs nanoparticles

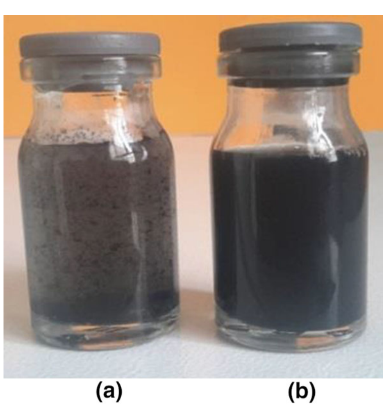

Fig. 5 Effect of surfactant on the nanofluid stability: **a** without CTAB; **b** with CTAB

$$U_{\mathrm{i,exp}} = \frac{Q_{\mathrm{avg}}}{A_{\mathrm{is,ip}} \times \mathrm{LMTD}} \tag{7}$$

Calculation steps for theoretical evaluation of overall heat transfer coefficient

Two Reynolds numbers are defined as:

$$\mathrm{Re_h} = \frac{\rho_\mathrm{h} \times V_\mathrm{h} \times D_\mathrm{h}}{\mu_\mathrm{h}}, \quad \mathrm{Re_c} = \frac{\rho_\mathrm{c} \times V_\mathrm{c} \times D_\mathrm{c}}{\mu_\mathrm{c}} \tag{8}$$

where D_c is hydraulic diameter of cold Water, V_c is velocity of cold water, V_h is velocity of hot fluid, μ_c is dynamic viscosity of cold water, and μ_h is dynamic viscosity of hot fluid. Density and specific heat of nanofluid are calculated from the following equations, respectively [39–42],

$$\rho_\mathrm{nf} = (\varphi \times \rho_\mathrm{p}) + (1 - \varphi)\rho_\mathrm{w} \tag{9}$$

$$C_\mathrm{p,nf} = \frac{\varphi \times (\rho_\mathrm{p} C_\mathrm{p,p}) + (1 - \varphi) \times (\rho_\mathrm{w} C_\mathrm{p,w})}{\rho_\mathrm{nf}} \tag{10}$$

Prandtl number of nanofluid is given by:

$$\mathrm{Pr_{nf}} = \frac{\mu_\mathrm{nf} \times C_\mathrm{p,nf}}{k_\mathrm{nf}} \tag{11}$$

k, ρ, C_p and μ for water are calculated at average temperature of water. Nusselt number for cold water is given by [43]:

$$\mathrm{Nu_c} = 3.657 + \frac{0.0677 \times \left(\mathrm{Re_c} \times \mathrm{Pr_c} \times \frac{D_\mathrm{c}}{L}\right)^{1.33}}{1 + (0.1 \times \mathrm{Pr_c}) \times \left(\mathrm{Re_c} \times \frac{D_\mathrm{c}}{L}\right)^{0.33}} \tag{12}$$

where

$$f = (1.82 \times \log_{10} \mathrm{Re_c} - 1.64)^{-2} \tag{13}$$

Nusselt number for hot fluid is given by [43]:

$$\mathrm{Nu_h} = \frac{\frac{f}{8} \times (\mathrm{Re_h} - 1000) \times \mathrm{Pr_h}}{1 + 12.7 \times \left\{\frac{f}{8}\right\}^{0.5} \times \left\{(\mathrm{Pr_h})^{0.666} - 1\right\}} \tag{14}$$

Two heat transfer coefficients will be defined: (1) heat transfer coefficient for the hot fluid inside the inner tube

(h_h) and (2) heat transfer coefficient for the coolant (h_c). They are defined as:

$$h_{\mathrm{h}} = \frac{\mathrm{Nu}_{\mathrm{h}} \times k_{\mathrm{h}}}{D_{\mathrm{h}}}, \quad h_{\mathrm{c}} = \frac{\mathrm{Nu}_{\mathrm{c}} \times k_{\mathrm{c}}}{D_{\mathrm{c}}} \tag{15}$$

Theoretical inner overall heat transfer coefficient is calculated by using of the following equation [43]:

$$U_{\mathrm{i,theo}} = \frac{1}{\frac{1}{h_{\mathrm{h}}} + \frac{d_{\mathrm{i,ip}}/2}{k_{\mathrm{ip}}} \times \ln\left\{\frac{d_{\mathrm{o,ip}}/2}{d_{\mathrm{i,ip}}/2}\right\} + \frac{d_{\mathrm{i,ip}}/2}{d_{\mathrm{o,ip}}/2} \times \frac{1}{h_{\mathrm{c}}}} \tag{16}$$

Analysis of the heat transfer characteristics

In this work, thermal conductivity of nanofluids was measured using a KD2-PRO thermal properties analyzer device. A Brookfield CAP 2000 viscometer measured the viscosity of nanofluids. Other thermophysical properties were estimated using correlations introduced in Eqs. 9–10 to verifying device results (KD2-PRO thermal properties analyzer device), thermal conductivity of pure water was obtained and compared with the results of the standard data of water.

Figure 6 shows the thermal conductivity ratios of MWCNTs–water nanofluids versus temperature at different concentrations. The results show a correlation between increasing thermal conductivity and increasing temperature and nanofluid mass concentration. A slightly increase is observed when the nanoparticles concentration fraction is increased and a maximum thermal conductivity enhancement was observed in the case of nanofluids containing mass% 0.25 MWCNTs. Similar trend has been previously reported in the literature conducted by Syam Sundar et al. [44]. This enhancement is mainly due to Brownian motions, inherent high thermal transfer properties and increased straightness ratio owing to the ball milling of the MWCNTs [45].

Figure 7 demonstrates the impact of temperature on the viscosity ratios (μ_{nf}/μ_{bf}) of MWCNT–water nanofluids. The viscosity of MWCNTs–water nanofluids decrease with increasing temperature and concentration, with the latter exerting stronger influence on the viscosity of nanofluids with different concentrations which may be attributed to the weakening of intermolecular forces. This observation corroborates the results of Hosseini et al. [46] and Aravind et al. [47] who observed that there is decrease in viscosity when the fluid temperature is increased. However, temperature has a stronger influence on the viscosity of nanofluids with different concentrations. The rather mild increase in the effective viscosity with nanoparticle concentration is a significance advantage since the increase in viscosity could undermine the overall positive impact of

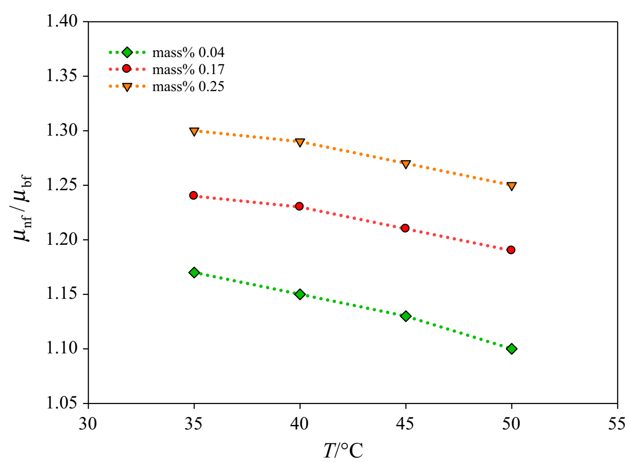

Fig. 7 Relative viscosity of MWCNTs–water nanofluids versus temperature at different concentrations

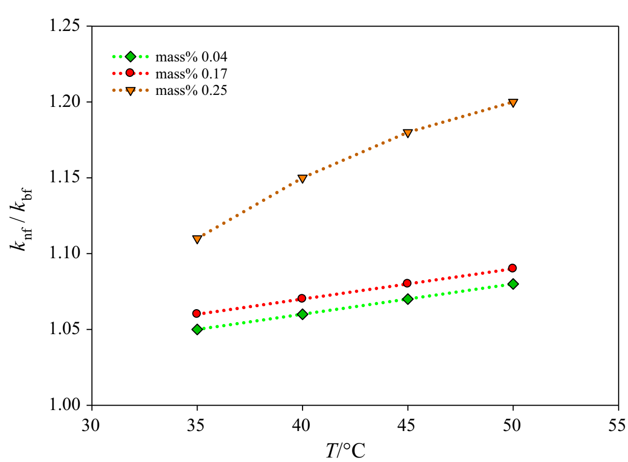

Fig. 6 Thermal conductivity ratios of MWCNTs–water nanofluids versus temperature at different concentrations

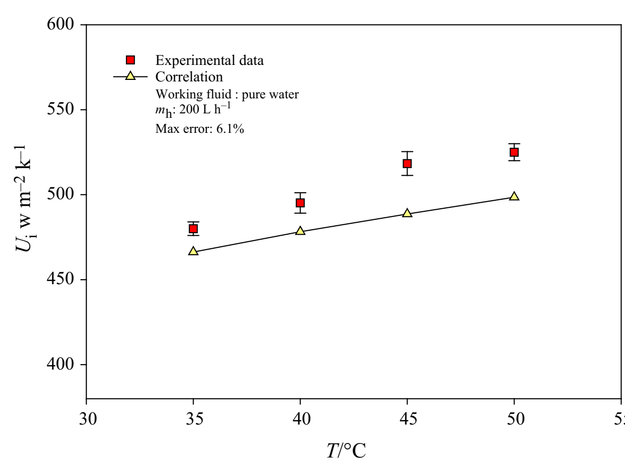

Fig. 8 Comparison between experimental and calculated value of inner overall heat transfer coefficient

enhanced conductivity in heat transfer due to the pumping fluid penalty [46].

Verification

To ensure the accuracy of the results, the overall heat transfer coefficient, U_i, of the pure water flow was compared with overall heat transfer coefficient in Eq. 16. Figure 8 shows the comparison between experimental and calculated values of inner overall heat transfer coefficient. As shown in Fig. 8, the results confer the validity of calculated versus experimental data. The uncertainty of the inner overall heat transfer coefficient measurement is approximately 6.1%. The results show a positive correlation between the inner overall heat transfer coefficient and with increasing temperatures. The maximum average enhancement for U_i is 16% for volume flow rate of 200 (L h^{-1}), at temperature of 50 °C.

Results and discussion

Heat transfer of nanofluids

Figure 9 demonstrates the relationships between the Nusselt number and the Reynolds number at different mass concentrations at the temperature of 50 °C. As illustrated, Nusselt number increases with the increasing Reynolds number and mass concentration of nanofluid. Moreover, Nusselt number of the nanofluid at the same Reynolds number is greater than the Nusselt number base fluid. For example, this value is 40% for the nanofluid with a concentration of 0.25 compared to the base fluid (the Reynolds number of 7600). This trend has been previously reported in the literature conducted by Sarafraz [18, 37]. Maximum variation occurs at Re=7600. The reason of increasing of Nusselt number with the increasing of mass concentration of nanoparticles is the increase in the thermal conductivity. The fluid velocity plays an important role on the heat transfer, and it is the main cause of give high heat transfer coefficient. The irregular and random movements of nanoparticles increase the energy exchange rates in the fluid with exerting shear stress on the walls and enhancing the thermal dispersion of the flow [48].

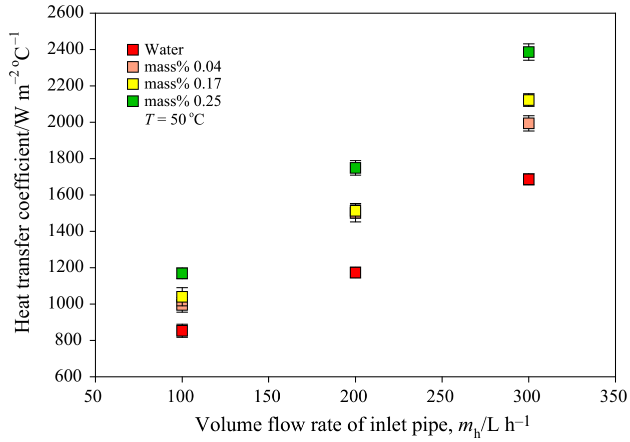

Fig. 10 Heat transfer coefficient versus volume flow rate of inlet pipe at different mass concentration of nanofluids at temperature of 50 °C

Figure 10 presents the results of experiments for heat transfer coefficient versus volume flow rate of inlet pipe at different mass concentration of nanofluids at temperature of 50 °C. Results demonstrate that, at higher volume flow rate of inlet pipe, the heat transfer coefficient increases. A similar trend can be seen for mass concentration, where increasing the mass concentration leads to an increase in the heat transfer coefficient. According to the results, with higher mass concentrations of MWCNT nanoparticles, the inlet temperature yields a higher heat transfer coefficient.

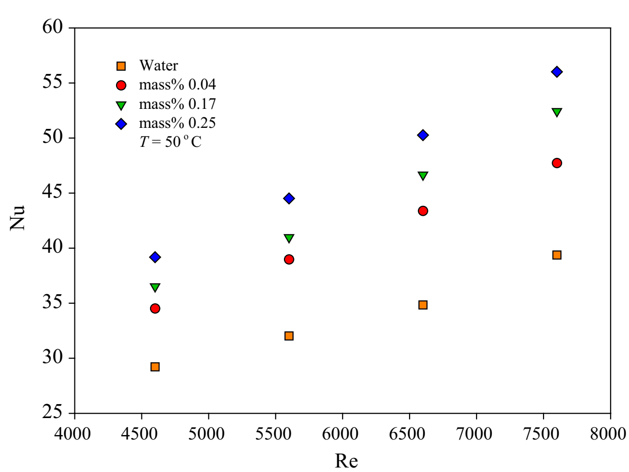

Fig. 9 Nusselt number versus Reynolds number at different mass concentration at the temperature of 50 °C

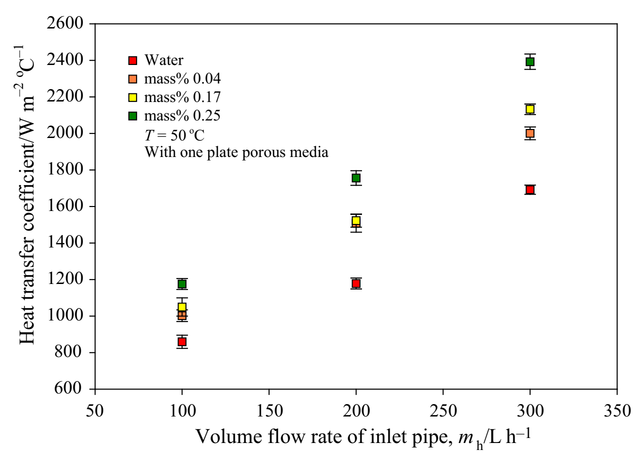

Fig. 11 Heat transfer coefficient versus volume flow rate of inlet pipe at different mass concentration of nanofluids under one-plate porous media

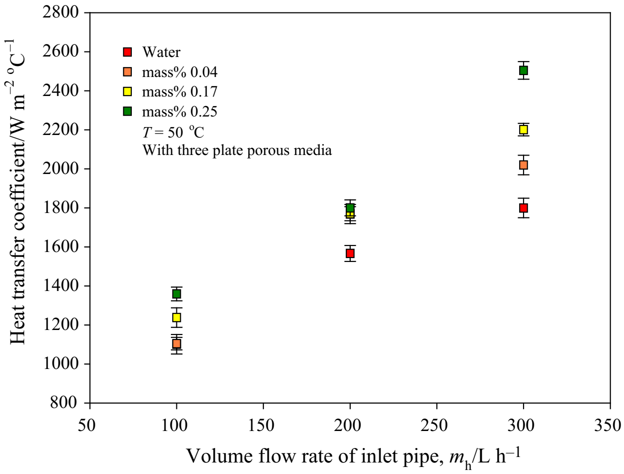

Fig. 12 Heat transfer coefficient versus volume flow rate of inlet pipe at different mass concentration of nanofluids under three-plate porous media

Porous media results

Figures 11 and 12 show the heat transfer coefficient versus volume flow rate of inlet pipe at different mass concentration of nanofluids under plate porous media conditions. It illustrates that the trend of variation is roughly the same as that shown in Fig. 10. As can be seen in Fig. 11, the enhancement in the heat transfer coefficient of nanofluid under one-plate porous media is insignificant.

Figure 12 shows the heat transfer coefficient versus volume flow rate at different mass concentration of nanofluids under the three-plate porous media. The enhancement in the heat transfer coefficient of nanofluid is approximately 10%, 19% and 16% for 0.04 mass%, 0.17 mass%, and 0.25 mass% in volume flow rate of 100 (L h^{-1}) compared to that of the absence of porosity, respectively. This is while the higher ranges have a slight influence on the heat transfer coefficient. At volume flow rate of 300 (L h^{-1}), the enhancement in the heat transfer coefficient approximately 1%, 3%, and 4% for 0.04 mass%, 0.17 mass%, and 0.25 mass%, respectively. This is because the heat transfer enhancement is dependent on the velocity of fluid flow more than any other factor. As can be seen, the heat transfer coefficient under three-plate porous media is enhanced in comparison to the one-plate porous media. It is evident that the application of porous media leads to the augmentation and enhancement of the mean heat transfer coefficient.

To better understand the effect of nanofluid and porous media on heat transfer performance, the ratio of the heat

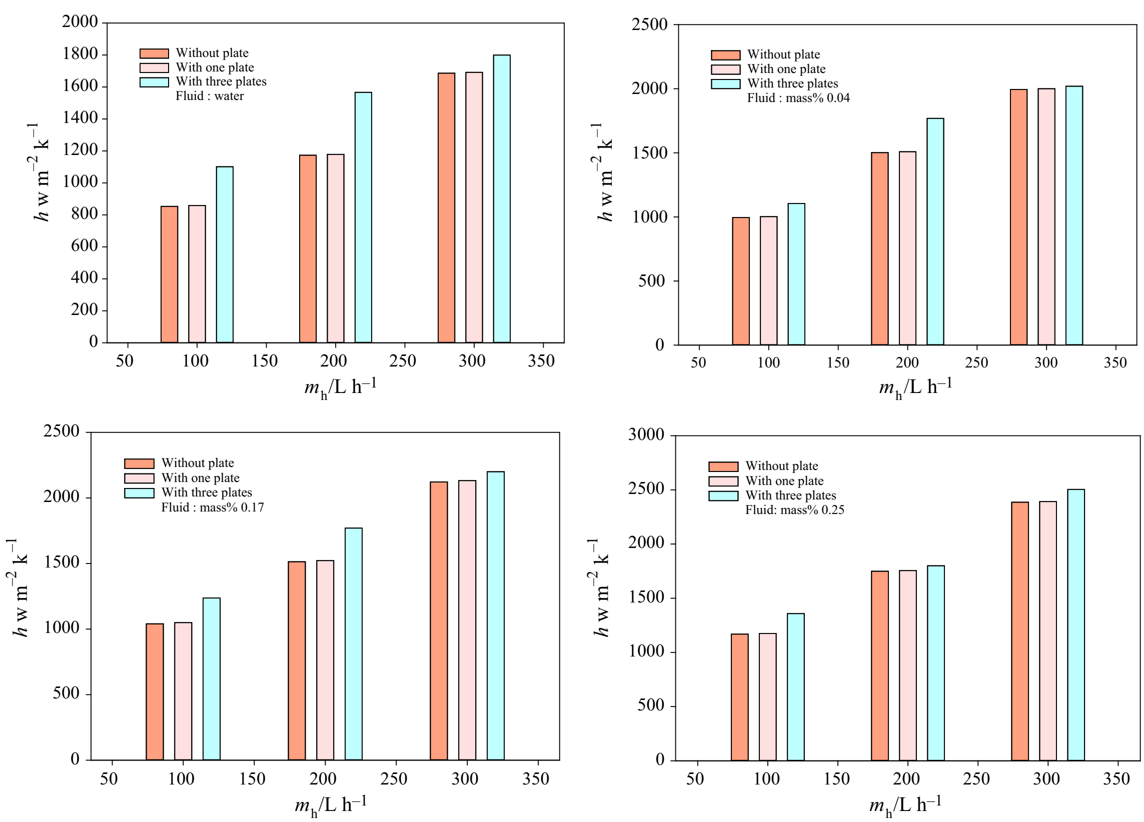

Fig. 13 Heat transfer coefficient versus volume flow rate under different conditions

transfer coefficient of nanofluid to heat transfer coefficient of pure water versus volume flow rate is plotted in Fig. 13. The experimental data of the heat transfer coefficient are reported for 0.04 mass%, 0.17 mass%, and 0.25 mass% In the absence of porosity the maximum heat transfer enhancement is obtained for nanofluid with 0.25 mass% fraction at 300 (L h^{-1}). This graph shows that the positive correlation between volume flow rate and heat transfer coefficient, as the volume flow rate increases the value of enhancement in the heat transfer coefficient gradually increases. According to the experimental data, the heat transfer coefficient values are clearly increased in porosity conditions, although this amount is too small for one plate but quite obvious for the three-plate situation. The greatest enhancement occurs for water fluid under three porous plate conditions, at approximately 35%. Also, the amount of enhancement decreases with increasing nanofluid concentration. This is due to the fact that with increasing the nanofluid concentration, the dynamic viscosity of nanofluid is increased which leads to increase in vibration damping. For high mass concentrations, increasing the fluid viscosity diminishes the vibration effects. The amount of heat transfer enhancement decreases slightly with increasing volume flow rate because the flow rate is the most effective factor on heat transfer enhancement which reduce the plate effects.

Conclusions

An experimental study was conducted to investigate the performance of double-tube counterflow heat exchanger under porous media conditions. The performance of heat exchanger was tested with MWCNTs–water nanofluid, with a focus on the influence of the volume flow rate and concentration of nanoparticles. The porous medium made of aluminum plate, employed throughout this experiment, with a large contact surface with the fluid and high thermal conductivity, enhanced the heat transfer. The enhancement coefficient increases dramatically with a porous tube surface. But the increase is observed to be dependent on the position of the characterization of flow intensity the lower range 100 (L h^{-1}) of the volume flow rate demonstrated a greater impact on the enhancement coefficient; while the higher ranges 300 (L h^{-1}) exhibited low influences. Using a single plate did not yield a significant impact the heat transfer coefficient, but using three plates had the highest heat transfer coefficient (up to 35%). And finally, there was a negative correlation between mass fractions and porous media enhancements, as the mass fractions increased, the value of porous media enhancement (on the heat transfer enhancement assisted by porous media) gradually decreased.

References

1. Afshari A, Akbari M, Toghraie D, Yazdi ME. Experimental investigation of rheological behavior of the hybrid nanofluid of MWCNT–alumina/water (80%)–ethylene-glycol (20%). J Therm Anal Calorim. 2018;132(2):1001–15. https://doi.org/10.1007/s10973-018-7009-1.
2. Mahian O, Kolsi L, Amani M, Estellé P, Ahmadi G, Kleinstreuer C, Marshall JS, Siavashi M, Taylor RA, Niazmand H, Wongwises S, Hayat T, Kolanjiyil A, Kasaeian A, Pop I. Recent advances in modeling and simulation of nanofluid flows—part I: fundamentals and theory. Phys Rep. 2018. https://doi.org/10.1016/j.physrep.2018.11.004 **(In Press)**.
3. Esfahani NN, Toghraie D, Afrand M. A new correlation for predicting the thermal conductivity of ZnO–Ag (50%–50%)/water hybrid nanofluid: an experimental study. Powder Technol. 2018;323:367–73.
4. Hemmat Esfe M, Hassani Ahangar MR, Toghraie D, Hajmohammad MH, Rostamian H, Tourang H. Designing artificial neural network on thermal conductivity of Al_2O_3–water–EG (60–40%) nanofluid using experimental data. J Therm Anal Calorim. 2016;126:837–43.
5. Lotfi R, Rashidi AM, Amrollahi A. Experimental study on the heat transfer enhancement of MWNT-water nanofluid in a shell and tube heat exchanger. Int Commun Heat Mass Transf. 2012;1:108–11. https://doi.org/10.1016/j.icheatmasstransfer.2011.10.002.
6. Duangthongsuk W, Wongwises S. Heat transfer enhancement and pressure drop characteristics of TiO_2–water nanofluid in a double-tube counter flow heat exchanger. Int J Heat Mass Transf. 2009;52(7):2059–67. https://doi.org/10.1016/j.ijheatmasstransfer.2008.10.023.
7. Hosseinnezhad R, Akbari OA, Afrouzi HH, Biglarian M, Koveiti A, Toghraie D. Numerical study of turbulent nanofluid heat transfer in a tubular heat exchanger with twin twisted-tape inserts. J Therm Anal Calorim. 2018;132(1):741–59. https://doi.org/10.1007/s10973-017-6900-5.
8. Rabienataj Darzi A, Farhadi M, Sedighi K. Heat transfer and flow characteristics of Al_2O_3–water nanofluid in a double tube heat exchanger. Int Commun Heat Mass Transf. 2013;47:105–12. https://doi.org/10.1016/j.icheatmasstransfer.2013.06.003.
9. Esfe MH, Hajmohammad H, Toghraie D, Rostamian H, Mahian O, Wongwises S. Multi-objective optimization of nanofluid flow in double tube heat exchangers for applications in energy systems. Energy. 2017;137:160–71. https://doi.org/10.1016/j.energy.2017.06.104.
10. Chun BH, Kang HU, Hyun Kim S. Effect of alumina nanoparticles in the fluid on heat transfer in double pipe heat exchanger system. Kor J Chem Eng. 2008;25:966–71. https://doi.org/10.1007/s11814-008-0156-5.
11. Aghayari R, Maddah H, Ashori F, Hakiminejad A, Aghili M. Effect of nanoparticles on heat transfer in mini double pipe heat exchangers in turbulent flow. Heat Mass Transf. 2013. https://doi.org/10.1007/s00231-014-1415-0.
12. Sadighi Dizaji H, Jafarmadar S, Mobadersani F. Experimental studies on heat transfer and pressure drop characteristics for new arrangements of corrugated tubes in a double pipe heat exchanger. Int J Therm Sci. 2015;96:211–20. https://doi.org/10.1016/j.ijthermalsci.2015.05.009.
13. Khedkar R, Sonawane SS, Wasewar KL. Heat transfer study on concentric tube heat exchanger using TiO_2–water-based nanofluid. Int Commun Heat Mass Transf. 2014. https://doi.org/10.1016/j.icheatmasstransfer.2014.07.011.
14. Bahiraei M, Hangi M. Investigating the efficacy of magnetic nanofluid as a coolant in double-pipe heat exchanger in the

presence of magnetic field. Energy Convers Manag. 2013;76:1125–33. https://doi.org/10.1016/j.enconman.2013.09.008.
15. Chandra Sekhara Reddy M, Vasudeva Rao V. Experimental investigation of heat transfer coefficient and friction factor of ethylene glycol water based TiO_2 nanofluid in double pipe heat exchanger with and without helical coil inserts. Int Commun Heat Mass Transf. 2014;50:68–76. https://doi.org/10.1016/j.icheatmasstransfer.2013.11.002.
16. Liu L, Kim E, Park YG, Jacobi AM. The potential impact of nanofluid enhancements on the performance of heat exchangers. Heat Transf Eng. 2012;33:31–41. https://doi.org/10.1080/01457632.2011.584814.
17. Ding Y, Alias H, Wen D, Williams RA. Heat transfer of aqueous suspensions of carbon nanotubes (CNTnanofluids). Int J Heat Mass Transf. 2005;49:240–50. https://doi.org/10.1016/j.ijheatmasstransfer.2005.07.009.
18. Sarafraz MM, Hormozi F, Nikkhah V. Thermal performance of a counter-current double pipe heat exchanger working with COOH–CNT/water nanofluids. Exp Thermal Fluid Sci. 2016;78:41–9. https://doi.org/10.1016/j.expthermflusci.2016.05.014.
19. Zadkhast M, Toghraie D, Karimipour A. Developing a new correlation to estimate the thermal conductivity of MWCNT-CuO/water hybrid nanofluid via an experimental investigation. J Therm Anal Calorim. 2017;129(2):859–67. https://doi.org/10.1007/s10973-017-6213-8.
20. Arabpour A, Karimipour A, Toghraie D. The study of heat transfer and laminar flow of kerosene/multi-walled carbon nanotubes (MWCNTs) nanofluid in the microchannel heat sink with slip boundary condition. J Therm Anal Calorim. 2018;131(2):1553–66. https://doi.org/10.1007/s10973-017-6649-x.
21. Alrashed AAA, Akbari OA, Heydari A, Toghraie A, Zarringhalam M, Shabani GAS, Seifi AR, Goodarzi M. The numerical modeling of water/FMWCNT nanofluid flow and heat transfer in a backward-facing contracting channel. Physica B. 2018;537:176–83. https://doi.org/10.1016/j.physb.2018.02.022.
22. Akhavan-Behabadi MA, Shahidi M, Aligoodarz MR, Fakoor-Pakdaman M. An experimental investigation on rheological properties and heat transfer performance of MWCNT-water nanofluid flow inside vertical tubes. Appl Therm Eng. 2016. https://doi.org/10.1016/j.applthermaleng.
23. Huang D, Wu Z, Sunden B. Pressure drop and convective heat transfer of Al_2O_3/water and MWCNT/water nanofluids in a chevron plate heat exchanger. Int J Heat Mass Transf. 2015;89:620–6. https://doi.org/10.1016/j.ijheatmasstransfer.2015.05.082.
24. Diao Y, Li CZ, Zhang J, Zhao Y, Kang Y. Experimental investigation of MWCNT–water nanofluids flow and convective heat transfer characteristics in multiport minichannels with smooth/micro-fin surface. Powder Technol. 2017;305:206–16. https://doi.org/10.1016/j.powtec.2016.10.011.
25. Karimipour-Fard P, Afshari E, Ziaei-Rad M, Taghian-Dehaghani S. A numerical study on heat transfer enhancement and design of a heat exchanger with porous media in continuous hydrothermal flow synthesis system. Chin J Chem Eng. 2017. https://doi.org/10.1016/j.cjche.2017.01.015.
26. Chamkha A, Rashad A, Aly A. Non-Darcy natural convection of a nanofluid about a permeable vertical cone embedded in a porous medium. Int J Microscale Nanoscale Therm Microscale Nanoscale Therm. 2012;4:99–114.
27. Bourantas G, Skouras E, Loukopoulos V. Heat transfer and natural convection of nanofluids in porous media. Eur J Mech B. 2014;43:45–56. https://doi.org/10.1016/j.euromechflu.2013.06.013.
28. Sheremet M, Pop I, Bachok N. Effect of thermal dispersion on transient natural convection in a wavy-walled porous cavity filled with a nanofluid: tiwari and Das' nanofluid model. Int J Heat Mass Transf. 2016;92:1053–60. https://doi.org/10.1016/j.ijheatmasstransfer.2015.09.071.
29. Uddin Z, Harmand S. Natural convection heat transfer of nanofluids along a vertical plate embedded in porous medium. Nanoscale Res Lett. 2013. https://doi.org/10.1186/1556-276x-8-64.
30. Armaghani T, Chamkha AJ, Maghrebi J, Nazari M. Numerical analysis of a nanofluid forced convection in a porous channel: a new heat flux model in LTNE condition. J Porous Media. 2014;17:637–46. https://doi.org/10.1615/JPorMedia.v17.i7.60.
31. Nasrin R, Alim MA, Chamkha AJ. Effect of the heating wall position on forced convection along two sided open enclosure with porous medium utilizing nanofluid. Int J Energy Technol Policy. 2013;5:1–13.
32. Nasrin R, Alim MA, Chamkha AJ. Numerical simulation of non-Darcy forced convection through a channel with non-uniform heat flux in an open cavity using nanofluid. Numer Heat Transf A. 2013;64:820–40. https://doi.org/10.1080/10407782.2013.798536.
33. Kasaeian A, Daneshazarian R, Mahian O, Kolsi L, Chamkha A, Wongwises S, Pop I. Nanofluid flow and heat transfer in porous media: a review of the latest developments. Heat and Mass Transf. 2017;107:778–91. https://doi.org/10.1016/j.ijheatmasstransfer.2016.11.074.
34. Pavel B, Pavel I, Abdulmajeed A. Mohamad, an experimental and numerical study on heat transfer enhancement for gas heat exchangers fitted with porous media. Int J Heat Mass Transf. 2005;47:4939–52. https://doi.org/10.1016/j.ijheatmasstransfer.2004.06.014.
35. Mohamad A. Heat transfer enhancements in heat exchangers fittedwith porous media part i: constant wall temperature. Int J Therm Sci. 2003;42:385–95. https://doi.org/10.1016/S1290-0729(02)00039-X.
36. Targui N, Kahalerras H. Analysis of fluid flow and heat transfer in a double-pipe heat exchanger with porous structures. Energy Convers Manag. 2008;49:3217–29. https://doi.org/10.1016/j.enconman.2008.02.010.
37. Sarafraz MM, Hormozi F. Intensification of forced convection heat transfer using biological nanofluid in a double-pipe heat exchanger. Exp Therm Fluid Sci. 2015;66:279–89. https://doi.org/10.1016/j.expthermflusci.2015.03.028.
38. Hosseinian A, Meghdadi Isfahani AH. Experimental study of heat transfer enhancement due to the surface vibrations in a flexible double pipe heat exchanger. Heat Mass Transf. 2017. https://doi.org/10.1007/s00231-017-2213-2.
39. Pak BC, Cho YI. Hydrodynamic and heat trans fer study of dispersed fluids with submicron metallic oxide particles. Exp Heat Transf. 1998;11:151–70. https://doi.org/10.1080/08916159808946559.
40. Heydari M, Toghraie D, Akbari OA. The effect of semi-attached and offset mid-truncated ribs and Water/TiO_2 nanofluid on flow and heat transfer properties in a triangular microchannel. Therm Sci Eng Prog. 2017;2:140–50. https://doi.org/10.1016/j.tsep.2017.05.010.
41. Pourfattah F, Motamedian M, Sheikhzadeh G, Toghraie D, Akbari OA. The numerical investigation of angle of attack of inclined rectangular rib on the turbulent heat transfer of Water-Al_2O_3 nanofluid in a tube. Int J Mech Sci. 2017;131:1106–16. https://doi.org/10.1016/j.ijmecsci.2017.07.049.
42. Esfe MH, Saedodin S, Mahian O, Wongwises S. Thermophysical properties, heat transfer and pressure drop of COOH-functionalized multi walled carbon nanotubes/water nanofluids. Heat Mass Transf. 2014. https://doi.org/10.1016/j.icheatmasstransfer.2014.08.037.

43. Chavda NK. effect of nanofluid on heat transfer characteristics of double pipe heat exchanger: part-II: effect of copper oxide nanofluid. Int J Res Eng Technol. 2015;4:688–96.
44. Syam Sundar L, Sharma KV, Singh MK, Sousa ACM. Hybrid nanofluids preparation, thermal properties, heat transfer and friction factor—a review. Renew Sustain Energy Rev. 2017. https://doi.org/10.1016/j.rser.2016.09.108.
45. Ganeshkumar J, Kathirkaman D, Raja K, Kumaresan V, Velraj R. Experimental study on density, thermal conductivity, specific heat, and viscosity of water-ethylene glycol mixture dispersed with carbon nanotubes. Therm Sci. 2017;21:255–65. https://doi.org/10.2298/tsci141015028g.
46. Hosseini M, Sadri R, Kazi SN, Bagheri S, Zubir N, Bee Teng C, Zaharinie T. Experimental study on heat transfer and thermophysical properties of covalently functionalized carbon nanotubes nanofluids in an annular heat exchanger: a green and novel synthesis. Energy Fuels. 2017;31:5635–44. https://doi.org/10.1021/acs.energyfuels.6b02928.
47. Aravind SJ, Baskar P, Baby TT, Sabareesh RK, Das S, Ramaprabhu S. Investigation of structural stability, dispersion, viscosity, and conductive heat transfer properties of functionalized carbon nanotube based nanofluids. J Phys Chem. 2011;34:16737–44.
48. Mohammed H, Hasan H, Wahid M. Heat transfer enhancement of nanofluids in a double pipe heat exchanger with louvered strip inserts. Int Commun Heat Mass Transf. 2013;40:36–46. https://doi.org/10.1016/j.icheatmasstransfer.2012.10.023.

Publisher's Note